Phytochemistry Letters 23 (2018) 141–148

Contents lists available at ScienceDirect

Phytochemistry Letters

journal homepage: www.elsevier.com/locate/phytol

Alkenyl cyclohexanone derivatives from *Lannea rivae* and *Lannea schweinfurthii*

Souaibou Yaouba[a], Andreas Koch[b], Eric M. Guantai[c], Solomon Derese[a], Beatrice Irungu[d], Matthias Heydenreich[b], Abiy Yenesew[a,*]

[a] Department of Chemistry, University of Nairobi, P.O. Box 30197-00100, Nairobi, Kenya
[b] Institut für Chemie, Universität Potsdam, Karl-Liebknecht-Str. 24-25, D-14476 Potsdam, Germany
[c] School of Pharmacy, University of Nairobi, P.O. Box 19676-00202, Nairobi, Kenya
[d] Centre for Traditional Medicine and Drug Research, Kenya Medical Research Institute, P.O. Box 54840-00200, Nairobi, Kenya

ARTICLE INFO

Keywords:
Lannea rivae
Lannea schweinfurthii
Alkenyl cyclohexenone
Alkenyl cyclohexanone
Anti-inflammatory
Cytotoxicity
Antimicrobial

ABSTRACT

Phytochemical investigation of the CH_2Cl_2/MeOH (1:1) extract of the roots of *Lannea rivae* (Chiov) Sacleux (Anacardiaceae) led to the isolation of a new alkenyl cyclohexenone derivative: (4*R*,6*S*)-4,6-dihydroxy-6-((*Z*)-nonadec-14′-en-1-yl)cyclohex-2-en-1-one (**1**), and a new alkenyl cyclohexanol derivative: (2*S**,4*R**,5*S**)-2,4,5-trihydroxy-2-((*Z*)-nonadec-14′-en-1-yl)cyclohexanone (**2**) along with four known compounds, namely epicatechin gallate, taraxerol, taraxerone and β-sitosterol; while the stem bark afforded two known compounds, daucosterol and lupeol. Similar investigation of the roots of *Lannea schweinfurthii* (Engl.) Engl. led to the isolation of four known compounds: 3-((*E*)-nonadec-16′-enyl)phenol, 1-((*E*)-heptadec-14′-enyl)cyclohex-4-ene-1,3-diol, catechin, and 1-((*E*)-pentadec-12′-enyl)cyclohex-4-ene-1,3-diol. The structures of the isolated compounds were determined by NMR spectroscopy and mass spectrometry. The absolute configuration of compound **1** was established by quantum chemical ECD calculations. In an antibacterial activity assay using the microbroth kinetic method, compound **1** showed moderate activity against *Escherichia coli* while compound **2** exhibited moderate activity against *Staphylococcus aureus*. Compound **1** also showed moderate activity against *E. coli* using the disc diffusion method. The roots extract of *L. rivae* was notably cytotoxic against both the DU-145 prostate cancer cell line and the Vero mammalian cell line (CC_{50} = 5.24 and 5.20 μg/mL, respectively). Compound **1** was also strongly cytotoxic against the DU-145 cell line (CC_{50} = 0.55 μg/mL) but showed no observable cytotoxicity (CC_{50} > 100 μg/mL) against the Vero cell line. The roots extract of *L. rivae* and *L. schweinfurthii*, epicatechin gallate as well as compound **1** exhibited inhibition of carageenan-induced inflammation.

1. Introduction

The genus *Lannea* (Anacardiaceae) comprises of about 40 species occurring in tropical Africa and Asia (Kokwaro, 1994). *Lannea rivae* (Chiov) Sacleux is a deciduous shrub or small tree with a flat spreading crown, widely distributed in Eastern Africa including Kenya, Uganda, Ethiopia and Tanzania (Kokwaro, 1994). The stem bark and roots of *L. rivae* are used to treat cough, cold and stomach-ache (Kipkore et al., 2014; Okoth et al., 2016). *Lannea schweinfurthii* (Engl.) Engl. is a small to medium-sized tree distributed in Kenya, Uganda, Tanzania, Malawi, Mozambique, Zambia, Zimbabwe, Swaziland and South Africa (Kindt et al., 2011; Kokwaro, 1994). Infusions of the roots of *L. schweinfurthii* are reported to enhance memory and are also used as a sedative (Seoposengwe et al., 2013). The roots of *L. schweinfurthii* have been reported to show very good radical scavenging activity and the plant was not toxic to human neuroblastoma SH-SY5Y cells at 100 μg/mL (Adewusia et al., 2013).

Lannea species elaborate tetracyclic and pentacyclic triterpenes, bifuran derivatives (Yun et al., 2014), phenolic lipids, alkyl cyclohexenol and alkyl cyclohexenone derivatives (Okoth and Koorbanally, 2015; Queiroz et al., 2003), tannins, benzoic acid derivatives (Islam et al., 2002; Kapche et al., 2007) and flavonoids (Islam and Tahara, 2000; Muhaisen, 2013; Okoth et al., 2013; Reddy et al., 2011; Sultana and Ilyas, 1986). Alkyl phenols, alkenyl cyclohexenones and other phytochemical constituents have been reported from *L. rivae* (Okoth et al., 2016), while the only report on *L. schweinfurthii* is on the biological activity of the crude extract (Adewusia et al., 2013).

In this study, the isolation and characterization of a new alkenyl cyclohexenone derivative (**1**) and a new alkenyl cyclohexanone derivative (**2**) from *L. rivae* along with six known compounds are reported.

* Corresponding author.
E-mail address: ayenesew@uonbi.ac.ke (A. Yenesew).

https://doi.org/10.1016/j.phytol.2017.12.001
Received 9 October 2017; Received in revised form 29 November 2017; Accepted 5 December 2017

Similar phytochemical studies of *L. schweinfurthii* led to the isolation of four known compounds. The anti-inflammatory, antimicrobial and cytotoxic activities of the crude extracts and some of the isolated compounds are also reported.

2. Results and discussion

Chromatographic separation of the CH_2Cl_2/MeOH (1:1) extract of the roots of *Lannea rivae* afforded a new alkenyl cyclohexenone derivative (**1**, Fig. 1), a new alkenyl cyclohexanone derivative (**2**) and four known compounds. The known compounds were identified as epicatechin gallate (Qi et al., 2003), taraxerol (Muithya, 2010), taraxerone (Muithya, 2010) and β-sitosterol (Chaturvedula and Prakash, 2012).

Compound **1** was isolated as a colourless paste; from HRESIMS ($[M + H]^+$ at *m/z* 393.3344) and NMR data (Table 1), the molecular formula $C_{25}H_{44}O_3$ was established. The presence of an α,β-unsaturated cyclohexenone moiety was evident from the UV (λ_{max} 256, 336 nm), and NMR spectral data (Table 1). The NMR spectra further showed that the cyclohexenone ring is substituted with two hydroxy, at C-4 (δ_H 4.62, δ_C 64.0) and C-6 (δ_C 74.5), and a C_{19} alkenyl (at C-6) group (Table 1). In the EIMS, the fragment ion at *m/z* 374 corresponding to $[M\text{-}H_2O]^+$ is in agreement with the presence of a hydroxy substituent (s). The identity of the alkenyl group as 14′-(*Z*)-nonadecenyl was deduced from the ^1H (δ_H 5.28 for H-14′/15′; δ_H 1.17 for H-3′-H-12′; δ_H 1.95 for H-13′/16′, and δ_H 0.83 for H-19) and ^{13}C (δ_C 129.8/129.7 for C-14′/15; δ_C 29.8-29.2 for C-3′-C-12′; δ_C 27.1 for C-13′; 26.8 for C-16′, and δ_C 13.9 for C-19′) NMR spectral data (Table 1). The HRMS which showed a protonated molecular ion peak at *m/z* 393.3344 is in agreement with a $C_{19}H_{37}$ alkenyl chain. The fragment ion at *m/z* 97 ($[C_7H_{13}]^+$) resulting from allylic cleavage of hep-2-en-1-ylium group is in agreement with the placement of the double bond at C-14′. The close ^{13}C NMR chemical shift values (δ_C 129.8 and 129.7) for the olefinic carbons C-14′ and C-15′ of **1** is consistent with the assignment of *Z*-configuration to the double bond in the alkenyl chain (David et al., 1998; Kapche et al., 2007; Okoth et al., 2016; Okoth and Koorbanally, 2015; Queiroz et al., 2003); in *E*-configured olefinic carbons (C-14′ and C-15′), the ^{13}C NMR resonances are expected to have substantially distinct values (Correia et al., 2006; Okoth and Koorbanally, 2015; Queiroz et al., 2003). The position of the double bond and its *Z*-configuration indicated that it is biosynthetically derived from the fatty acid [5ω]-hexadecenoic-*cis*-hexadecenoic acid, through a similar mechanism as proposed for related compounds (Correia et al., 2006).

The substitution pattern in the cyclohexenone ring was established from the HMBC experiment (Table 1), whereby ^3J correlation of H-2 (δ_H 5.96) with C-4 (δ_C 64.0) and C-6 (δ_C 74.5), H-3 (δ_H 6.80) with C-1 (δ_C 200.9) and C-5 (δ_C 41.0), and CH_2-5 (δ_H 2.20 and 2.15) with C-1 and C-3 were observed. The placement of the alkenyl group at C-6 was also supported by the HMBC correlation of CH_2-1′ (δ_H 1.71) with C-1 (δ_C 200.9) and C-5 (δ_C 41.0), as observed in related compounds (Okoth et al., 2016).

Table 1
^1H (800 MHz) and ^{13}C (200 MHz) NMR data of **1** in $CDCl_3$.

Position	δ_H (J in Hz)	δ_C (ppm)	HMBC (H → C)
1	–	200.9	–
2	5.96 (d, *J* = 10.1)	126.6	C-3, C-4, C-6
3	6.80 (dd, *J* = 3.6, 10.1)	149.4	C-1, C-5
4	4.62 (m)	64.0	C-2, C-5, C-6
5	2.20 (dd, *J* = 5.4, 14.2)	41.0	C-1, C-3
	2.15 (dd, *J* = 5.4, 14.2)		C-1, C-3
6	–	74.5	–
1′	1.72 (m)	39.0	C-1, C-5, C-3′
2′	1.25 (m)	22.9	C-3′
3′ – 12′	1.17 (br s)	29.8–29.2	C-3′-C-12′, C-13′
13′	1.95 (m)	27.1	C-12′, C-15′
14′,15′	5.28 (t, *J* = 4.8)	129.8, 129.7	C-13′, C-16′
16′	1.95 (m)	26.8	C-14′, C-18′
17′	1.25 (m)	31.8	C-15′, C-19′
18′	1.25 (m)	22.2	C-16′, C-19′
19′	0.83 (m)	13.9	C-17′

The planar structure of this compound is the same as the ones reported by Okoth et al. (2016) and de Jesus Correia et al. (2001). On the basis of NMR evidence, these authors proposed (4*S**,6*S**)-**1** and (4*S**,6*R**)-**1** relative configuration, respectively. Here, in determining the absolute configuration in compound **1**, firstly, the energies of different conformations for (4*S**,6*S**)-**1a** and (4*S**,6*R**)-**1a**, where the side chain at C-6 is shorter (to reduce computational time) were calculated and the conformations with minimum energy in each case identified. In the case of (4*S**,6*R**)-**1a,** two conformations with ΔE = 0.14 Kcal/mol were considered (Fig. 3, Boltzmann weighted: 55.1 for conformation I and 44.9% for II, respectively). Hydrogen-bonding between 4-OH and 6-O (in conformation I, Fig. 3) and between 6-OH and C═O (in conformation II, Fig. 3) may be responsible for the stabilities of these conformers. Furthermore, it can be seen that the 5-CH_2 group in conformation I is 'down', while in conformation II this group is 'up' with respect to the other ring carbon atoms which are almost span a plane. From these calculations it is apparent that the cyclohexenone ring is not rigid, undergoing ring flipping between conformations I and II (Fig. 3); consequently the ^3J values (5.4 Hz) observed between H-4 and both protons at C-5 is a mean value (which is in good agreement with calculated value, Table 2), indicating that coupling constant and NOE interactions could not be used for conformational or configurational analyses to determine the relative configuration with certainty. It follows then that the configurational assignments proposed by Roumy et al. (2009), Okoth et al. (2016) and de Jesus Correia et al. (2001), on the basis of NMR evidence with the assumption of stable cyclohexenone ring, may not be reliable.

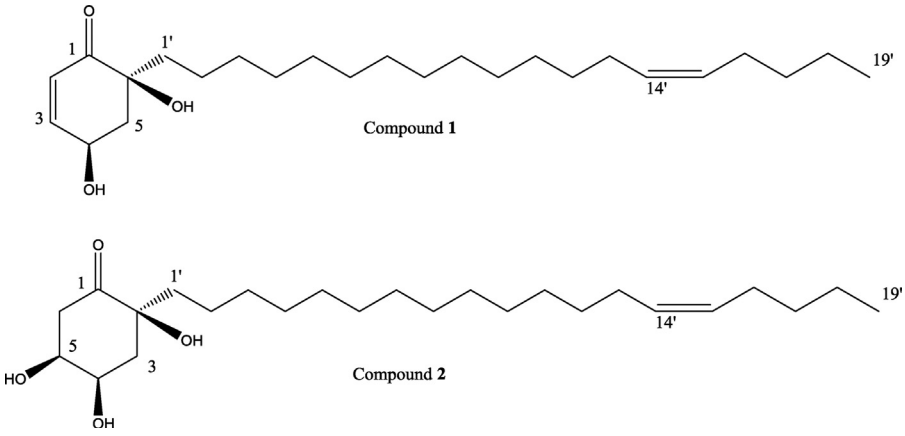

Fig. 1. Structures of compounds **1** and **2.**

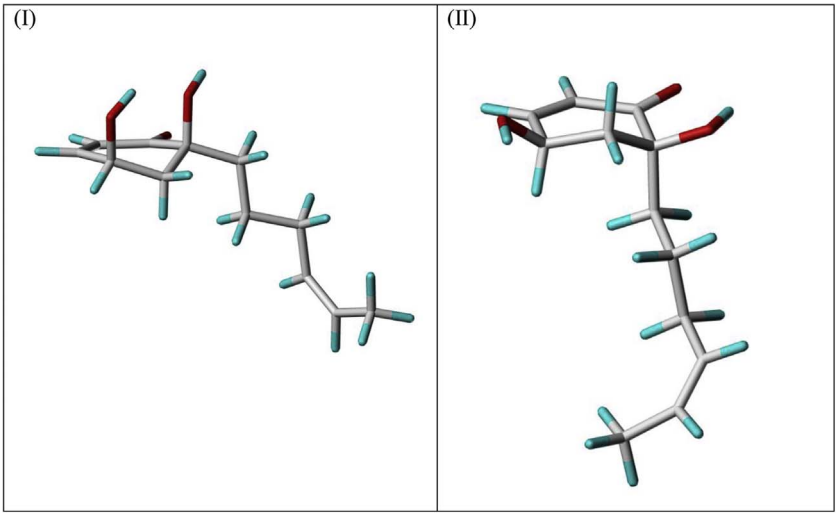

Fig. 2. The calculated global energy minimum geometries of conformers of (4*R*,6*S*)-**1a** (conformation I: global minimum, conformation II: + 0.14 kcal/mol).

The experimental ECD spectrum of compound **1** (Fig. 3a), which showed negative Cotton effect at λ_{max} 337 nm, was then compared with the computed ECD spectra for stable conformers of (4*S*,6*S*)-**1a**, (4*R*,6*R*)-**1a**, (4*R*,6*S*)-**1a** and (4*S*,6*R*)-**1a**. Of these, the best match was obtained for (4*R*,6*S*)-**1a** isomer where two conformations with low energies (I and II, Fig. 2) showed negative Cotton effects at 360, 335 nm, respectively (Fig. 3b). In fact the ECD spectrum of the weighed sum of these conformers is in a close match with the experimental ECD (Fig. 3a). In order to explain the long wave length absorption position in the computed ECD spectrum of conformation I (360 nm), the most important π-π* and π,n-π* electron transitions were calculated and were found to be between donor MO's 54–56 and LUMO at 270 nm and between donor MO's 56 and 57 and LUMO at 358 nm (Fig. 4). The latter one is highly influenced by the π electron system of the exocyclic double bond which transfers electrons into the LUMO which is essentially situated at the double bond of the 2-cyclohexenone ring system (Fig. 4). However, the length of the side chain was shortened during calculations for practical reasons. Thus, the calculated wavelength may differ slightly from the actual one of (4*R*,6*S*)-**1** and may overlap with n-π* transitions from the 2-cyclohexenone ring system which are known to be in the range of approximately 330–340 nm. However, here the sign of the Cotton effect is much more influenced by the orientation of the 4-OH group than that of the long-chain substituent at position 6 which is much weaker (Kwit et al., 2010). It follows then that the configurational assignment discussed above is reliable and consequently compound **1** was characterized as (4*R*,6*S*)-4,6-dihydroxy-6-((*Z*)-nonadec-14′-en-1-yl)cyclohex-2-en-1-one.

The second new compound (**2**) was isolated as a colourless paste from the roots of *Lannea rivae*. EIMS analysis showed a weak molecular ion peak at *m/z* 410 and a more stable fragment ion at *m/z* 392 for $[M-H_2O]^+$. Comparison of the MS and NMR data of this compound (Table 3) with those of compound **1** (M^+ 392, NMR: Table 1) indicated that compound **2** could be a hydro-derivative of **1** with a molecular formula $C_{25}H_{46}O_4$. The UV (λ_{max} 206 nm) spectrum and ^{13}C NMR chemical shift value of the carbonyl (δ_C 210.9 for C═O) did not show an α,β-unsaturated carbonyl as in compound **1**, rather the presence of a cyclohexanone ring in compound **2** was evident from the NMR spectra (Table 3). The NMR spectral data further showed that the cyclohexanone ring is substituted with three hydroxy groups, at C-2 (δ_C 77.3), C-4 (δ_C 68.5; δ_H 4.20) and C-5 (δ_C 71.9; δ_H 4.00) and a long alkenyl chain at C-2 (Table 3). The substitution pattern in the cyclohexanone ring was established from the HMBC spectrum: correlation of CH_2-3 (δ_H 2.98 and 2.78) with C-1 (δ_C 210.9) and C-5 (δ_C 71.4); H-4 (δ_H 4.20) with C-2 (δ_C 77.3) and C-6 (δ_C 40.4); H-5 (δ_H 4.00) with C-1 (δ_C 210.9) and C-3; CH_2-6 (δ_H 2.40 and 1.72) with C-2 and C-4; and CH_2-1′ (δ_H 1.79 and 2.06) with C-1 and C-3. This substitution pattern was further supported by H,H—COSY (CH_2-3↔H-4↔H-5↔CH_2-6) spectrum. This observation

Table 2
Theoretically calculated coupling constants ($^3J_{4H-5H}$) for different conformations of (4*R*,6*S*)-**1a** using the Haasnoot-de Leeuw-Altona equation (Altona, 1996).

Conformation	Dihedral angle[a]	*J* (in Hz)
I	H4-H5α (46°)	3.9
	H4-H5β (−72°)	1.9
II	H4-H5α (−53°)	5.1
	H4-H5β (−170°)	11.1
Weighted mean values (I and II)	H4-H5α	4.4
	H4-H5β	5.9
Experimental[b]	H4-H5α	5.4
	H4-H5β	5.4

[a] from theoretically calculated conformations of **1a**.
[b] for compound **1**.

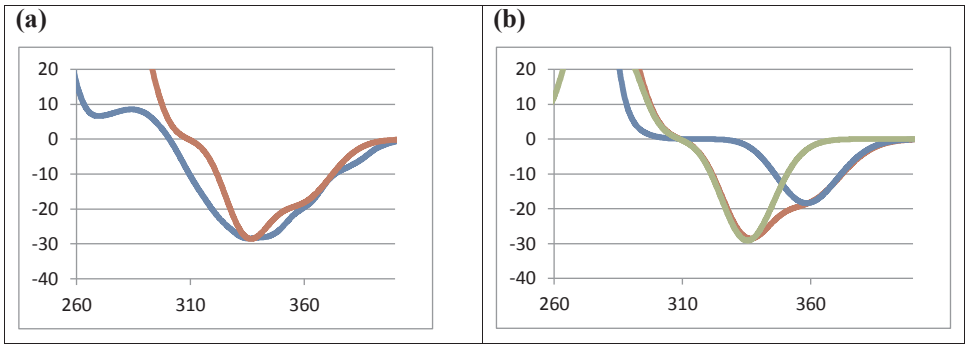

Fig. 3. ECD spectra of compound **1** (exp.) and (4*R*,6*S*)-**1a** (calc.): (a) blue experimental, red Boltzmann weighted sum of calculated CD's for conformations I and II (55.9 and 44.1%, resp.); (b) calculated CD's, red Boltzmann weighted sum of conformations I and II, blue conformation I, and green conformation II. (For interpretation of the references to colour in this figure legend, the reader is referred to the web version of this article.)

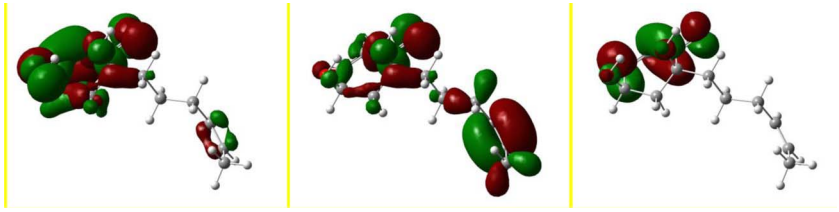

Fig. 4. Donor MO's 54–56 (left), donor MO's 56 and 57 (middle), and LUMO (MO 58, right) of conformation I of (4*R*,6*S*)-**1a**.

Table 3
^{1}H (600 MHz) and ^{13}C (150 MHz) NMR data of **2** in CD_2Cl_2.

Position	δ_H (J in Hz)	δ_C (ppm)	HMBC(H → C)
1	–	210.9	–
2	–	77.3	–
3	2.98 (dd, *J* = 11.2, 12.3, H-3ax)	41.8	C-1, C-5
	2.70 (m, H-3eq)		C-1, C-2, C-4, C-5
4	4.20 (ddd, *J* = 3.1, 4.5, 11.0)	68.5	C-2, C-3, C-6
5	4.00 (m)	71.9	C-1, C-3
6	2.40 (dd, *J* = 4.1, 14.8, H-6a)	40.4	C-1, C-2, C-4, C-5
	1.71 (dd, *J* = 3.5, 14.8, H-6b)		C-2, C-4
1′	2.06 (m)	39.5	C-1, C-3
	1.77 (d, *J* = 4.4)		C-1, C-3
2′	1.36 (m)	23.1	C-3′
3′–12′	1.29 (br s)	29.8–29.3	C3′-C12′, C-13′
13′	2.06 (m)	27.2	C-14′, C-15′
14′, 15′	5.36 (m)	129.8, 129.7	C-13′, C-16′
16′	2.06 (m)	26.9	C-14′, C-18′
17′	1.36 (m)	32.0	C-15′, C-19′
18′	2.06 (m)	22.4	C-16′, C-19′
19′	0.94 (t, *J* = 7.1)	13.7	C-17′, C-18′

indicated that two of the hydroxy groups are located on adjacent carbon atoms, at C-4 and C-5.

The NMR spectral data of **2** was similar to that of the compound previously identified from the same plant, *Lannea rivae* (Okoth et al., 2016), except on the length of the side chain and that the configuration of the compound reported by Okoth et al. (2016) has not been determined. The side chain at C-2 in compound **2** was established to be nonadec-14-en-1-yl group from MS ($[M]^+$ at *m/z* 410) and NMR spectral data (Table 3). As in compound **1**, the fragment ion at *m/z* 97 ($[C_7H_{13}]^+$) formed as the result of allylic cleavage of hept-2-en-1-ylium group is consistent with the placement of the double bond at C-14′. The HMBC spectrum showed correlation of CH_3-19′ (δ_H 0.94) with the sp^3 carbon atoms, C-17′ (δ_C 32.0) and C-18′ (δ_C 22.4), showing that the double bond is not located two bonds away from the terminal methyl group as found in some other alkenyl cyclohexenone derivatives (Okoth and Koorbanally, 2015; Queiroz et al., 2003). The HMBC correlation of H-13′ (δ_H 2.06) and H-16′ (δ_H 2.06) with C-14′ (δ_C 129.7) and C-15′ (δ_C 129.8), confirmed the placement of the double bond at C-14′. Comparison of the ^{1}H and ^{13}C NMR data with those of compound **1** and related compounds having similar long alkenyl chain suggested a *Z*-geometry at C-14′ (Groweiss et al., 1997; Kapche et al., 2007; Okoth and Koorbanally, 2015). The two olefinic protons on the side chain, H-14′ and H-15′, appeared as overlapping resonances at δ_H 5.39 (t, *J* = 4.7 Hz) showing HMBC correlations with the allylic carbon resonances at δ_C 26.9 (C-13′) and δ_C 27.2 (C-16′). These ^{13}C NMR chemical shift values are consistent with a *Z*-configuration for the double bond on the side chain, as allylic carbon atoms in *E*-configured double bonds are expected to appear at higher resonance values (*ca.* δ_C 32.0) (Roumy et al., 2009).

The large coupling constant between Hax-3 (δ_H 2.98, 1H, *dd*, *J* = 12.3, 11.2 Hz) and H-4 (δ_H 4.20, *ddd*, *J* = 11.0, 4.5, 3.1 Hz) requires that H-4 is also axial, and hence OH-4 should be equatorial. On the other hand, the small coupling constant between H-4 and H-5 requires that H-5 is equatorial, making OH-5 to be axially oriented. These observations are consistent with the two hydroxy groups being *cis*-oriented. The co-occurrence of compound **2** with **1** indicated that they are biogenetically related, and it is likely that the configurations at C-2 (C-6 in compound **1**) and C-4 in compound **2** are the same as in **1**. In compound **2** (where the cyclohexanone ring is rigid, stabilized by hydrogen bonding between C=O and OH-2), OH-4 being equatorial (β-oriented), OH-5 should be axial (β-oriented). Thus, the relative configuration of **2** is likely to be (2*S**,4*R**,5*S**). Hence the compound was characterized as (2*S**,4*R**,5*S**)-2,4,5-trihydroxy-2-((*Z*)-nonadec-14′-en-1-yl)cyclohexanone. An isomeric compound, (2*S*,4*R*,5*R*)-2,4,5-trihydroxy-2-((*Z*)-nonadec-14′-en-1-yl)cyclohexanone has been described in a Chinese patent (Chengbin et al., 2006).

Similar investigation of the stem bark extract of *Lannea rivae* led to the isolation of two known compounds: daucosterol (Khatun et al., 2012) and lupeol (Abdullahi et al., 2013). Investigation of the roots of *Lannea schweinfurthii* led to the isolation of taraxerol (Muithya, 2010), taraxerone (Muithya, 2010), lupeol (Abdullahi et al., 2013), 3-((*E*)-nonadec-16′-enyl)phenol (Okoth and Koorbanally, 2015) and 1-((*E*)-pentadec-12′-enyl)cyclohex-4-ene-1,3-diol. Analysis of the extract of the stem bark of *L. schweinfurthii* also led to the isolation of the known compounds 3-((*E*)-nonadec-16′-enyl)phenol (Okoth and Koorbanally, 2015), 1-((*E*)-heptadec-14′-enyl)cyclohex-4-ene-1,3-diol (Okoth and Koorbanally, 2015), catechin (Qi et al., 2003) and 1-((*E*)-pentadec-12′-enyl)cyclohex-4-ene-1,3-diol.

2.1. Anti-inflammatory assay

The crude extracts of the roots of *Lannea rivae* and *Lannea schweinfurthii*, the compounds (4*R*,6*S*)-4,6-dihydroxy-6-((*Z*)-nonadec-

Table 4
Anti-inflammatory activity – inhibition of carrageenan-induced paw oedema of crude extracts and compounds of *Lannea* species.

Treatment/Sample	Dose (mg/kg)	Increase in paw volumes (mL) (mean ± SD, n = 4)				
		0 mn	60 min	120 min	180 min	240 min
LRR[a] extract	200	0	1.17 ± 0.07	1.20 ± 0.04	1.17 ± 0.04	1.60 ± 0.03
LSR[b] extract	200	0	1.10 ± 0.04	1.16 ± 0.09	1.15 ± 0.03	1.25 ± 0.09
1	200	0	1.24 ± 0.03	1.21 ± 0.06	1.13 ± 0.03	1.43 ± 0.02
Epicatechin gallate	200	0	1.17 ± 0.07	1.17 ± 0.03	1.17 ± 0.05	1.35 ± 0.11
Normal saline	–	0	1.29 ± 0.07	1.32 ± 0.19	1.57 ± 0.13	1.62 ± 0.08
Indomethacin	10	0	0.84 ± 0.01	0.95 ± 0.04	0.97 ± 0.01	1.03 ± 0.02

[a] LRR = *Lannea rivae* roots.
[b] LSR = *Lannea schweinfurthii* roots.

14′-en-1-yl)cyclohex-2-en-1-one (**1**) and epicatechin gallate were evaluated for *in vivo* anti-inflammatory activities at 200 mg/kg using indomethacin as the standard anti-inflammatory drug. As shown in Table 4, the extracts and the compounds tested showed moderate inhibition of carrageenan-induced paw oedema, though none were as active as indomethacin. The *L. schweinfurthii* roots extract was the most active at 60 and 120 min post-carrageenan administration, and showed the smallest increase in paw volume observed at any time point (+ 1.10 mL). However, compound **1** was the most active at 180 min after carrageenan administration, suggesting a delayed onset of maximal effect for this compound. The observed *in vivo* anti-inflammatory activity of *L. rivae* and *L. schweinfurthii* extracts of the roots partially support the reported traditional use of *Lannea* species for the relief of pain and inflammation (Okoth et al., 2016; Okoth and Koorbanally, 2015). Furthermore, compound **1** and epicatechin gallate could be some of the constituent phytochemicals that contribute towards the observed *in vivo* anti-inflammatory activity of the extracts.

2.2. Antimicrobial assay

Some of the isolates, including the new compounds **1** and **2**, were tested for antimicrobial activity against *Staphylococcus aureus* and *Escherichia coli* using the microbroth kinetic method. Compound **1**, taraxerol, β-sitosterol, taraxerone and lupeol showed moderate activities against *E. coli*, while only compound **2** and β-sitosterol showed activity against *S. aureus* (Table 5A). Compound **1**, epicatechin gallate and the crude extract of *Lannea rivae* were also assayed for their antibacterial activity against *S. aureus*, *E. coli* and several fungal species using the disc diffusion method. Epicatechin gallate showed high activity against *E. coli* with a zone of inhibition comparable to that of the standard drug gentamicin (Table 5B), which is in agreement with literature reports (Gibbons et al., 2004; Okoth et al., 2016; Park et al., 2004; Sakanaka et al., 2000). Compound **1** also showed moderate activity against *E. coli*, which corroborated the results from the microbroth kinetic assay for this compound. No activity was observed against *S. aureus* or any of the fungal strains. Previous studies have also shown that β-sitosterol has antibacterial activity against several bacterial strains including *S. aureus* and *E. coli* (Odiba et al., 2014). The antibacterial activities of lupeol, taraxerol and β-sitosterol have also been reported in literature (Salleh et al., 2016).

Table 6
Cytotoxicity of of some of the isolated compounds and extracts of *Lannea* species against mammalian cell lines.

Sample	CC_{50} (μg/mL)	
	Vero cell lines	DU-145 cell lines
LRR[a] extract	5.20 ± 0.01	5.24 ± 0.12
LSR[b] extract	7.36 ± 0.03	74.00 ± 0.04
1	> 100	0.55 ± 0.08
Epicatechin gallate	> 100	> 100
Taraxerone	> 100	11.00 ± 0.07
β-Sitosterol	> 100	> 100
3-((*E*)-nonadec-16'-enyl)phenol	16.14 ± 0.01	49.76 ± 0.10

[a] LRR = *Lannea rivae* roots.
[b] LSR = *Lannea schweinfurthii* roots.

2.3. Cytotoxicity assay

The cytotoxicity of compound **1**, epicatechin gallate, taraxerone, β-sitosterol,

3-((*E*)-nonadec-16′-enyl)phenol, *Lannea rivae* and *Lannea schweinfurthii* roots extracts against the DU-145 prostate cancer cell line and Vero cell line was tested (Table 6). Compound **1** was strongly cytotoxic against DU-145 prostate cancer cell line with a CC_{50} value of 0.55 μg/mL. The crude extract of the roots of *L. rivae* and taraxerone were also

Table 5
Results of antimicrobial assays of compounds of *Lannea* species.

A. Microbroth kinetic system

Samples	*E. coli* (NCTC 7447)			*S. aureus* (NCTC 12923)		
	160[a]	80	40	160	80	40
	% Inhibition			% Inhibition		
1	56.64	59.44	25.64	ne	ne	ne
2	na	ne	ne	na	43.56	42.38
Taraxerol	31.93	33.33	37.06	ne	ne	ne
β-Sitosterol	52.44	53.84	na	na	28.69	14.20
Taraxerone	34.49	29.83	28.43	ne	ne	ne
Lupeol	45.68	31.93	29.37	ne	ne	ne
1-((*E*)-heptadecen-14'-yl)-cyclohex-4-en-1,3-diol	ne	ne	ne	ne	ne	ne
3-((*E*) nonadecen-16'-yl)phenol	na	ne	ne	na	ne	ne
Gentamicin (standard)	61.51	53.08	50.28	95.60	96.55	96.94
Erythromycin (standard)	41.01	7.30	ne	98.08	97.89	98.08

B. Disc diffusion test method

		E. coli (ATCC 25922)	*S. aureus* (ATCC 25923)
	Amount per disc (μg)	Inhibition zone in mm	
1	150	9	0
Epicatechin gallate	100	20	0
LRR extract[b]	150	0	0
Gentamycin (standard)	0.6	20	13

Notes: *Antifungal test carried out on compound* **1**, *epicatechin gallate and the crude extract of* the roots of *Lannea rivae against clinical isolates of Microsporum gypseum, Trichophyton mentagrophytes and Cryptococcus neoformans, environmental isolates of Aspergilus flavus and Aspergilus niger, as well as standard strains of Candida parapsilosis (ATCC 22019) and Candida albicans (ATCC 90018) did not show any activity.*

[a] Concentration (μg/ml); *na = not assessed, ne = not effective.*
[b] LRR = *Lannea rivae* roots.

notably cytotoxic against the DU-145 cell line (CC_{50} = 5.24 and 11.00 μg/mL, respectively). *L. rivae* roots extract was found to be the most cytotoxic against the Vero cell line (CC_{50} = 5.20 μg/mL) followed by *L. schweinfurthii* roots extract (CC_{50} = 7.36 μg/mL). Among the pure compounds tested, only 3-((*E*)-nonadec-16′-enyl)phenol showed significant activity against the Vero cell line, exhibiting a CC_{50} value of 16.14 μg/mL. Epicatechin gallate and β-sitosterol were not cytotoxic against either of the cell lines.

Cytotoxicity of epicatechin gallate against a panel of mammalian cell lines has been previously reported (Babich et al., 2005; Kurbitz et al., 2011; Weisburg et al., 2004); however in this study the compound did not show cytotoxicity (CC_{50} > 100 μg/mL) against the DU-145 and Vero cell lines. Previous *in vitro* studies indicated that β-sitosterol inhibits the growth and simulates the apoptosis of MDA-MB-231 human breast cancer cells (Jassbi et al., 2016). Cyclohexenone derivatives such as 3-((*E*)-nonadec-16′-enyl)phenol, having different alkenyl side chains have been reported to exhibit high *in vitro* cytotoxic activity against the Chinese hamster ovarian cell line (Okoth and Koorbanally, 2015). A compound similar to **2** with different configuration and side chain showed strong cytotoxicity against Chinese hamster ovarian cell-lines (Okoth et al., 2016). Compound **1,** 3-((*E*)-nonadec-16′-enyl)phenol and taraxerone have showed cytotoxicity, and appear to contribute to cytotoxicity of the crude extracts (Table 6).

3. Experimental section

3.1. General

UV spectra were measured using a Shimadzu UV–vis spectrometer-2700. NMR spectra were acquired on Bruker Avance II 600 and Bruker Avance III HD 800 spectrometers, using the residual solvent peaks as reference. The spectra were processed using MestReNova 10.0 software. Coupling constants (*J*) were given in Hz. EI-MS was determined by direct inlet, 70 eV on Micromass GC-TOF micro mass spectrometer (Micromass, Wythenshawe, Waters Inc., UK). ECD spectra were recorded on a J-815 CD-spectropolarimer, serial No. Ao30261168. Optical rotations were measured on a PerkinElmer 341-LC Polarimeter. TLC analyses were carried out on glass plates of 20 × 20 cm dimension, pre-coated with silica gel $60F_{254}$ having 0.25 to 1 mm thickness. Column chromatography was run on silica gel 60 Å (70–230 mesh). Gel filtration was performed on sephadex LH-20.

3.2. Plant materials

Lannea rivae and *Lannea schweinfurthii* were collected from Ngong forest, Kenya in July 2014. The plants were identified by Mr Patrick B.C. Mutiso of the Herbarium, School of Biological Sciences, University of Nairobi, where voucher specimens *L. rivae* (SY2014/01) and *L. schweinfurthii* (SY2014/02) were deposited.

3.3. Extraction and isolation of compound from Lannea rivae

The air-dried and ground roots (850 g) of *Lannea rivae* was extracted with CH_2Cl_2/MeOH (1:1), 4 × 24 h, by percolation at room temperature. The solvent was evaporated using a rotary evaporator to give 180.9 g of a brown crude extract. A portion of the crude extract (175.0 g) was partitioned between CH_2Cl_2 and H_2O, then between EtOAc and H_2O. Removal of the organic solvents gave a CH_2Cl_2 (7.8 g) and EtOAc (34.0 g) extracts. The CH_2Cl_2 extract (7.8 g) was subjected to column chromatography on silica gel (80 g) eluting with *n*-hexane containing increasing amounts of EtOAc. The fractions eluted with 15% EtOAc in *n*-hexane were combined and further separated by column chromatography on sephadex LH-20 (eluent: CH_2Cl_2/CH_3OH, 1:1) to give **1** (210 mg) and **2** (83 mg). The fractions eluted with 10% EtOAc in *n*-hexane were combined and further separated by column chromatography on silica gel using *n*-hexane and EtOAc (4:1) to give taraxerol (56 mg), taraxerone (47 mg) and β-sitosterol (95 mg). The EtOAc extract (34 g) was subjected to column chromatography on silica gel (500 g) using *n*-hexane-EtOAc system and fractions eluted with 20% EtOAc in *n*-hexane were combined and purified on sephadex LH-20 (eluent: CH_2Cl_2/CH_3OH, 1:1) to afford epicatechin gallate (460 mg) and taraxerol (105 mg).

The powdered stem bark (980 g) of *Lannea rivae* was also extracted and partitioned as described above to give CH_2Cl_2 (7.9 g) and EtOAc (51 g) extracts. The CH_2Cl_2 extract was chromatographed on silica gel (200 g) and eluted with *n*-hexane containing increasing amounts of EtOAc. The elution with 10% EtOAc in *n*-hexane gave 3-((*E*)-nonadec-16'-enyl)phenol (17 mg). The EtOAc extract was also subjected to column chromatography on silica gel (500 g) using *n*-hexane-EtOAc as solvent system. The fractions obtained by elution with 4–6% EtOAc in *n*-hexane were combined and purified on sephadex LH-20 (eluent: CH_2Cl_2/CH_3OH, 1:1) to give daucosterol (89 mg) and lupeol (130 mg).

3.4. Extraction and isolation of compounds from Lannea schweinfurthii

The powdered roots (1.9 kg) of *Lannea schweinfurthii* was extracted with CH_2Cl_2/MeOH (1:1) as described above to give 156.7 g of crude extract. A portion of the crude extract (150.0 g) was partitioned between CH_2Cl_2 and H_2O (1:1) to afford 3.2 g of CH_2Cl_2 extract. The water layer was then extracted with EtOAc to yield 61.0 g of the EtOAc extract. The EtOAc extract was subjected to CC on silica gel (550 g) eluted with *n*-hexane containing increasing amounts of EtOAc to give three major fractions. Separation of the fraction eluted with 20% EtOAc in *n*-hexane was further purified by CC over sephadex LH-20 (eluent: CH_2Cl_2/CH_3OH, 1:1) to afford catechin (42 mg) and 1-((*E*)-pentadec-12′-enyl)cyclohex-4-ene-1,3-diol (46 mg). The CH_2Cl_2 extract (3.2 g) was also subjected to column chromatography on silica gel (50 g) eluted with *n*-hexane containing increasing amounts of EtOAc. Taraxerol (21 mg) and 3-((*E*)-nonadec-16′-enyl)phenol (27 mg) were obtained from the fractions eluted with 18% and 20% EtOAc in *n*-hexane, respectively. The fraction eluted with 25% EtOAc in *n*-hexane was subjected to further purification on sephadex LH-20 (eluent: CH_2Cl_2/MeOH, 1:1) to give 1-((*E*)-heptadec-14′-enyl)cyclohex-4-ene-1,3-diol (54 mg).

The powder stem bark (2 kg) of *L. schweinfurthii* was also extracted and partitioned as described above to obtain EtOAc and CH_2Cl_2 extracts. The EtOAc extract (56.8 g) was subjected to column chromatography on silica gel (550 g) using *n*-hexane-EtOAc system as eluent. β-sitosterol (39 mg) and lupeol (16 mg) were again isolated when eluting the column with 15% EtOAc in *n*-hexane. The fraction obtained with 30% EtOAc in *n*-hexane were combined and subjected to further purification on sephadex LH-20 (eluent: CH_2Cl_2/MeOH, 1:1) to afford 1-((*E*)-pentadec-12′-enyl)cyclohex-4-ene-1,3-diol (17 mg). The CH_2Cl_2 faction from the roots extract of *L. schweinfurthii* led to the isolation of more amounts of taraxerol (31 mg) and β-sitosterol (15 mg).

3.5. Physical and spectroscopic data of compounds 1 and 2

(4R,6S)-4,6-Dihydroxy-6-((Z)-nonadec-14′-en-1-yl)cyclohex-2-en-1-one (**1**). Colourless residue, $[\alpha]_D^{20}$ + 28.8° (*c* 0.5, acetone). UV λ_{max} (MeOH): 256, 336 nm. ^1H and ^{13}C NMR ($CDCl_3$): Table 1. EIMS *m/z* (rel. int.): 392 (6, $[M]^+$), 374 (14, $[M\text{-}H_2O]^+$), 97 (23, $[C_7H_{13}]^+$), 95 (35), 84 (100), 69 (25), 55 (52), 43 (31). HRESIMS $[M + H]^+$ *m/z*: 393.3344 ($C_{25}H_{45}O_3$ calcd. for 393.3369).

(2S,4R*,5S*)-2,4,5-Trihydroxy-2-((Z)-nonadec-14′-en-1-yl)cyclohexanone* (**2**). Colourless residue, $[\alpha]_D^{20}$ + 4.8° (*c* 0.6, acetone). UV λ_{max} (MeOH) 206 nm. ^1H and ^{13}C NMR (CD_2Cl_2): Table 3. EIMS *m/z* (rel. int.): 410 (4, $[M]^+$), 392 (20, $[M\text{-}H_2O]^+$), 390 (40), 374 (17, $[M\text{-}2H_2O]^+$), 339 (21), 337 (100), 139 (49), 99 (16), 97 (35, $[C_7H_{13}]^+$), 57 (33), 55 (62), 43 (12).

3.6. Cytotoxicity assay

Cytotoxic activity was evaluated using the 3-(4,5-dimethylthiazol-2-yl)-2,5-diphenyltetrazolium bromide (MTT) assay as previously described (Irungu et al., 2014). The colorimetric MTT cytotoxicity assay was based on the ability of mitochondrial oxidoreductase enzymes within viable mammalian cells to cleave the tetrazolium ring of the pale yellow MTT and thereby form dark blue formazan crystals, which are largely impermeable to cell membranes and accumulate within viable cells. The amount of generated formazan is directly proportional to the number of viable cells, thereby affording an indirect way of quantifying the proportion of viable mammalian cells under different experimental conditions (Irungu et al., 2014).

The MTT assay was carried out as previously described (Irungu et al., 2014) using the mammalian African monkey kidney (Vero) and DU-145 prostate cancer cell lines. Briefly, the cells were maintained in continuous culture in Eagle's Minimum Essential Medium (MEM) supplemented with 10% fetal bovine serum (FBS). The assays were carried out on varying concentrations of the test compounds in 96 well plates. Percentage cell viability in each well was estimated by solubilizing the formazan crystals in DMSO and determining the absorbance at 570 nm using a microtitre plate reader. Using the absorbance data, percentage cell viability for each concentration of test compound was calculated relative to the untreated wells. This dose-response data was then analysed using nonlinear regression to yield the corresponding concentration required for 50% inhibition of cell viability (CC_{50}) for each of the test compounds.

3.7. In vivo anti-inflammatory assay

In vivo evaluation of the anti-inflammatory activity of isolated compounds and extracts was carried out using the carrageenan-induced rat paw edema method (Tarkang et al., 2015). Twenty eight adult Wistar rats were randomly divided into seven groups. Hind paw volumes were recorded for each rat using a Mercury plethysmograph, applying the Archimedes principle of fluid displacement. Ten (10) mg/kg of vehicle (normal saline), the standard drug indomethacin (10 mg/kg) and 200 mg/kg body weight of each isolated compound or extract were administrated orally to different groups of rats. After thirty minutes, paw edema was induced in each rat by injecting 0.1 mL of carrageenan (1% in normal saline) into the right hind paw. Paw volumes were determined and recorded at 60, 120, 180 and 240 min after carrageenan administration. The difference between the paw volume before induction of edema and at each time point was taken as a measure of edema. Evaluation of anti-inflammatory activity was done by comparison of the paw volumes in treated groups with those of the untreated group.

3.8. In vitro anti-microbial assay

Two complementary test methods, namely microbroth kinetic method (using 40, 80 and 160 µg/mL test concentrations) and disc diffusion method (using 100 and 150 µg/disc) were used for antimicrobial evaluation of extracts and selected compounds against *Escherichia coli* (NCTC 7447, ATCC 25923) and *Staphylococcus aureus* (NCTC 12923, ATCC 25922) as described previously (Esma et al., 2009), using gentamicin and erythromycin as positive controls. The antifungal activities of compound **1**, epicatechin gallate and the crude extract of *Lannea rivae* were also tested against clinical isolates of *Microsporum gypseum, Trichophyton mentagrophytes* and *Cryptococcus neoformans*, environmental isolates of *Aspergilus flavus* and *Aspergilus niger*, as well as standard strains of *Candida parapsilosis* (ATCC 22019) and *Candida albicans* (ATCC 90018) using disc diffusion method as described previously (Nikkon et al., 2003; Valgas et al., 2007).

3.9. Theoretical calculation

Different conformations and configurations of the studied compound with a reduced chain length were optimized at the B3LYP/6-311G** (Becke, 1993) level of theory without any restrictions. The CD were computed using the Time Dependent DFT (TDDFT) (Autschbach et al., 2002; Bauernschmitt and Ahlrichs, 1996) algorithm in the program package GAUSSIAN 09 (Frisch et al., 2009). The 6–31G* basis set was applied. 10 singlet and 10 triplet states were solved (keyword TD (NStates = 10; 50-50). All GAUSSIAN results were analysed and the spectra displayed using the SpecDis 1.62 (Bruhn et al., 2014). The molecules are displayed using SYBYL-X 2.1.1 (SYBYL-X 2.1.1, 2013).

Acknowledgements

SY acknowledges the support of AFIMEGQ intra-ACP project for the PhD fellowship. The International Science Program (ISP Sweden, grant no KEN-02) is acknowledged for financial support. We are thankful to Mr Patrick B. Chalo Mutiso, of the School of Biological Sciences, University of Nairobi, Kenya, for the identification of the plant material. We are grateful to the Director of National Quality and Control Laboratory (NQCL), Nairobi Hospital, Kenya, for access to the laboratory to carry out the antibacterial assay.

Appendix A. Supplementary data

Supplementary data associated with this article can be found, in the online version, at https://doi.org/10.1016/j.phytol.2017.12.001.

References

Abdullahi, S., Musa, A., Abdullahi, M., Sule, M., Sani, Y., 2013. Isolation of lupeol from the stem-bark of *Lonchocarpus sericeus* (Papilionaceae). Sch. Acad. J. Biosci. 1, 18–19.
Adewusia, E.A., Foucheb, G., Steenkamp, V., 2013. Effect of four medicinal plants on amyloid-β induced neurotoxicity in SH-SY5Y cells. Afr. J. Tradit. Comp. Altern. Med 10, 6–11.
Altona, C., 1996. In: Grant, D.M., Morris, R. (Eds.), Encyclopedia of NMR. Wiley, New York, USA, pp. 4909—4923.
Autschbach, J., Ziegler, T., van Gisbergen, S.J., Baerends, E.J., 2002. Chiroptical properties from time-dependent density functional theory. I. Circular dichroism spectra of organic molecules. J. Chem. Phys. 116, 6930–6940.
Babich, H., Krupka, M.E., Nissim, H.A., Zuckerbraun, H.L., 2005. Differential in vitro cytotoxicity of (−)-epicatechin gallate (ecg) to cancer and normal cells from the human oral cavity. Toxicol. In Vitro 19, 231–242.
Bauernschmitt, R., Ahlrichs, R., 1996. Treatment of electronic excitations within the adiabatic approximation of time dependent density functional theory. Chem. Phys. Lett. 256, 454–464.
Becke, A.D., 1993. Density-functional thermochemistry III. The role of exact exchange. J. Chem. Phys 98, 5648–5652.
Bruhn, T., Schaumlöffel, A., Hemberger, Y., Bringmann, G., 2014. SpecDis, Version 1.62. University of Wuerzburg, Germany.
Chaturvedula, V.S.P., Prakash, I., 2012. Isolation of stigmasterol and β-sitosterol from the dichloromethane extract of *Rubus suavissimus*. Int. Curr. Pharm. J. 1, 239–242.
Chengbin C, Changwei L., Bing C., Bing H., Isolation of polysubstituted saturated cyclohexanone compounds as antitumor agents. From Faming Zhuanli Shenqing 2006, CN 187238 A 20061206. 2006.
Correia, S.D.J., David, J.P., David, J.M., 2006. Secondary metabolites from species of Anacardiaceae. Quim. Nova 29, 1287–1300.
David, J.M., Chávez, J.P., Chai, H.-B., Pezzuto, J.M., Cordell, G.A., 1998. Two new cytotoxic compounds from *Tapirira guianensis*. J. Nat. Prod. 61, 287–289.
de Jesus Correia, S., David, J.M., David, J.P., Chai, H.B., Pezzuto, J.M., Cordell, G.A., 2001. Alkyl phenols and derivatives from *Tapirira obtusa*. Phytochemistry 56, 781–784.
Esma, G.K., Özbilge, H., Albayrak, S., 2009. Determination of the effect of gentamicin agains: *Staphylococcus aureus* by using microbroth kinetic system. Ankem. Derg. 23, 110–114.
Frisch, M., Trucks, G., Schlegel, H., Scuseria, G., Robb, M., Cheeseman, J., Petersson, G., Fox, D.J., 2009. Gaussian 09, Revision A 02. Gaussian Inc., Wallingford, CT.
Gibbons, S., Moser, E., Kaatz, G.W., 2004. Catechin gallates inhibit multidrug resistance (mdr) in Staphylococcus aureus. Planta Med. 70, 1240–1242.
Groweiss, A., Cardellina, J.H., Pannell, L.K., Uyakul, D., Kashman, Y., Boyd, M.R., 1997. Novel cytotoxic: alkylated hydroquinones from Lannea welwitschii. J. Nat. Prod. 60, 116–121.
Irungu, B.N., Orwa, J.A., Gruhonjic, A., Fitzpatrick, P.A., Landberg, G., Kimani, F., Midiwo, J., Erdélyi, M., Yenesew, A., 2014. Constituents of the roots and leaves of Ekebergia capensis and their potential antiplasmodial and cytotoxic activities.

Molecules 19, 14235–14246.
Islam, M.T., Ito, T., Sakasai, M., Tahara, S., 2002. Zoosporicidal activity of polyflavonoid tannin identified in lannea coromandelica stem bark against phytopathogenic oomycete aphanomyces cochlioides. J. Agric. Food Chem. 50, 6697–6703.
Islam, M.T., Tahara, S., 2000. Dihydroflavonols from lannea coromandelica. Phytochemistry 54, 901–907.
Jassbi, A.R., Firuzi, O., Miri, R., Salhei, S., Zare, S., Zare, M., Masroorbabanari, M., Chandran, J.N., Schneider, B., Baldwin, I.T., 2016. Cytotoxic activity and chemical constituents of *Anthemis mirheydari*. Pharm. Biol. 54, 2044–2049.
Kapche, G., Laatsch, H., Fotso, S., Kouam, S., Wafo, P., Ngadjui, B., Abegaz, B., 2007. Lanneanol: a new cytotoxic dihydroalkylcyclohexenol and phenolic compounds from Lannea nigritana (Sc Ell.) Keay. Biochem. Syst. Ecol. 35, 539–543.
Khatun, M., Billah, M., Quader, M.A., 2012. Sterols and sterol glucoside from Phyllanthus species. Dhaka Univ. J. Sci. 60, 5–10.
Kindt, R., van Breugel, P., Lillesø, J., Bingham, M., Demissew, S., Dudley, C., Friis, I., Gachathi, F., Kalema, J., Mbago, F., 2011. Potential Natural Vegetation of Eastern Africa: Volume 2. Forest and Landscape, pp. 1–62 Working Paper.
Kipkore, W., Wanjohi, B., Rono, H., Kigen, G., 2014. A study of the medicinal plants used by the marakwet community in Kenya. J. Ethnobiol. Ethnomed. 10, 1–22.
Kokwaro, J.O., 1994. Flowering plant families of East Africa: an introduction to plant taxonomy. East Afr. Educ. Publ. 292.
Kurbitz, C., Heise, D., Redmer, T., Goumas, F., Arlt, A., Lemke, J., Rimbach, G., Kalthoff, H., Trauzold, A., 2011. Epicatechin gallate and catechin gallate are superior to epigallocatechin gallate in growth suppression and anti-inflammatory activities in pancreatic tumor cells. Cancer Sci. 102, 728–734.
Kwit, M., Gawronski, J., Boyd, D.R., Sharma, N.D., Kaik, M., 2010. Circular dichroism: optical rotation and absolute configuration of 2-cyclohexenone-cis-diol type phenol metabolites: redefining the role of substituents and 2-cyclohexenone conformation in electronic circular dichroism spectra. Org. Biomol. Chem. 8, 5635–5645.
Muhaisen, H.M., 2013. Chemical constituents from the bark of Lannea acida A: Rich. (Anacardiaceae). Der. Pharm. Chem. 5, 88–96.
Muithya, J.N., 2010. Phytochemical and in Vitro Anti-microbial Screening of Eechinops Hispidus Fresen. and Grewia Similis K. Schum. (PhD). School of Pure and Applied Science, Kenyatta University, Nairobi Kenya, pp. p109.
Nikkon, F., Saud, Z.A., Rehman, M., Haque, M.E., 2003. In vitro antimicrobial activity of the compound isolated from chloroform extract of *Moringa oleifera* Lam. Pak. J. Biol. Sci. 22, 1888–1890.
Odiba, J., Musa, A., Hassan, H., Yahay, S., Okolo, E., 2014. Antimicrobial activity of isolated stigmast-5-en-3-β-ol (β-sitosterol) from honeybee propolis from north-western, Nigeria. Int. J. Pharma. Sci. Res. 5, 908–918.
Okoth, D.A., Akala, H.M., Johnson, J.D., Koorbanally, N.A., 2016. Alkyl phenols: alkenyl cyclohexenones and other phytochemical constituents from Lannea rivae (Chiov.) Sacleux (Anacardiaceae) and their bioactivity. Med. Chem. Res. 25, 690–703.
Okoth, D.A., Chenia, H.Y., Koorbanally, N.A., 2013. Antibacterial and antioxidant activities of flavonoids from Lannea alata (Engl.) Engl. (Anacardiaceae). Phytochem. Lett. 6, 476–481.
Okoth, D.A., Koorbanally, N.A., 2015. Cardanols, long chain cyclohexenones and cyclohexenols from Lannea schimperi (Anacardiaceae). Nat. Prod. Commun. 10, 103–106.
Park, K.D., Park, Y.S., Cho, S.J., Sun, W.S., Kim, S.H., Jung, D.H., Kim, J.H., 2004. Antimicrobial activity of 3-O-acyl-(−)-epicatechin and 3-O-acyl-(+)-catechin derivatives. Planta Med. 70, 272–276.
Qi, S.H., Wu, D.G., Ma, Y.B., Luo, X.D., 2003. A novel flavane from Carapa guianensis. Acta Bot. Sin. 45, 1129–1132.
Queiroz, E.F., Kuhl, C., Terreaux, C., Mavi, S., Hostettmann, K., 2003. New dihydroalkylhexenones from *Lannea edulis*. J. Nat. Prod. 66, 578–580.
Reddy, A.K., Joy, J.M., Kumara, C.A., 2011. J. Pharm. Res. 4, 577–579. Available online through www.Jpronline.Info.
Roumy, V., Fabre, N., Portet, B., Bourdy, G., Acebey, L., Vigor, C., Valentin, A., Moulis, C., 2009. Four anti-protozoal and anti-bacterial compounds from Tapirira guianensis. Phytochemistry 70, 305–311.
Sakanaka, S., Juneja, L.R., Taniguchi, M., 2000. Antimicrobial effects of green tea polyphenols on thermophilic spore-forming bacteria. J. Biosci. Bioeng. 90, 81–85.
Salleh, W.M.N.H.W., Ahmad, F., Yen, K.H., Zulkifli, R.M., 2016. Chemical constituents and bioactivities from the leaves of Beilschmiedia glabra. Marmara Pharm. J. 20, 401–407.
Seoposengwe, K., van Tonder, J.J., Steenkamp, V., 2013. In vitro neuroprotective potential of four medicinal plants against rotenone-induced toxicity in SH-SY5Y neuroblastoma cells. BMC Comp. Altern. Med. 13, 2–11.
Sultana, S., Ilyas, M., 1986. A flavanone from *Lannea acida*. Phytochemistry 25, 963–964.
SYBYL-X 2.1.1, 2013. Tripos a Certara Company. (1699 South Hanley Rd., St. Louis, MO).
Tarkang, P.A., Okalebo, F.A., Siminyu, J.D., Ngugi, W.N., Mwaura, A.M., Mugweru, J., Agbor, G.A., Guantai, A.N., 2015. Pharmacological evidence for the folk use of Nefang: antipyretic: anti-inflammatory and antinociceptive activities of its constituent plants. BMC Complement. Altern. Med. 15, 11–12.
Valgas, C., Souza, S.M.d., Smânia, E.F., Smânia, Jr.A., 2007. Screening methods to determine antibacterial activity of natural products. Br. J. Microbiol 38, 369–380.
Weisburg, J.H., Weissman, D.B., Sedaghat, T., Babich, H., 2004. In vitro cytotoxicity of epigallocatechin gallate and tea extracts to cancerous and normal cells from the human oral cavity. Basic Clin. Pharmacol. Toxicol. 95, 191–200.
Yun, X.J., Shu, H.M., Chen, G.Y., Ji, M.H., Ding, J.Y., 2014. Chemical constituents from barks of *Lannea coromandelica*. Chin. Herb. Med. 6, 65–69.